

Influence of the Counteranion on the Formation of Polymeric Networks by Metal Complexes of Hexamethylenebis(acetamide)

Nicholas P. Chatterton, David M. L. Goodgame,* David A. Grachvogel, Izhar Hussain, Andrew J. P. White, and David J. Williams*

Department of Chemistry, Imperial College of Science, Technology and Medicine, London SW7 2AY, U.K.

Received June 20, 2000

An investigation into the anion dependence of the network-forming ability of metal complexes of hexamethylenebis(acetamide), $\text{CH}_3\text{CONH}(\text{CH}_2)_6\text{NHCOCH}_3$ (HMBA), has resulted in the X-ray characterization of the compounds $[\text{Co}(\text{HMBA})_3][\text{Co}(\text{NCS})_4]$, **1**, $[\text{Nd}(\text{HMBA})_3][\text{Nd}(\text{NO}_3)_6] \cdot 2\text{CHCl}_3$, **2**, $[\text{Co}(\text{HMBA})_3][\text{HgCl}_4]$, **3**, and $[\text{Mn}(\text{HMBA})_3][\text{HgBr}_4] \cdot 3\text{CHCl}_3$, **4**. The structures of compounds **1**, **3**, and **4** each comprise cationic frameworks formed by the bridging action of HMBA ligands binding octahedrally to the cobalt or manganese centers and, in the cases of **3** and **4**, the formation of tetrahedral HgX_4^{2-} anions by transfer of the respective halide ions from Co or Mn to Hg. Complete anion (NO_3^-) transfer between Nd centers is also a key factor in the structure of **2**, which forms a cationic 3-D network of HMBA-bridged octahedrally coordinated Nd centers with occluded $[\text{Nd}(\text{NO}_3)_6]^{3-}$ anions. These types of inter-metal-anion transfer, with consequent complex counteranion formation, appear to facilitate the network-forming ability of the metal–HMBA cationic arrays.

Introduction

We have recently shown by X-ray crystallography that the polymethylenebis(amides) $\text{CH}_3\text{CONH}(\text{CH}_2)_n\text{NHCOCH}_3$ ($n = 2, 4, 6$) readily form polymeric network structures with manganese(II) and cobalt(II).¹ In the case of hexamethylenebis(acetamide) ($n = 6$; HMBA) the chloride and bromide complexes form large rhomboidal “boxes” by a process of halide ion transfer from one metal center to another, resulting in compounds of the type $\{[\text{M}(\text{HMBA})_3][\text{MX}_4]\}_n$. The cationic framework in these compounds is generated by the bridging action of HMBA molecules binding octahedrally via the oxygen atoms of the amide groups, with the tetrahedral MX_4^{2-} anions occupying the interstices of the rhomboidal boxes thus formed. In contrast, the polymers formed by butylenebis(acetamide) ($n = 4$; BBA) and by ethylenebis(acetamide) ($n = 2$; EBA) take the form of sheet networks of stoichiometry $\{[\text{M}(\text{BBA})_3]\text{X}_2\}_n$ and $\{[\text{M}(\text{EBA})_2(\text{H}_2\text{O})_2]\text{X}_2\}_n$, respectively, in which the anions remain as simple halide ions and are located between the sheets.

Although we could, at least in part, rationalize these changes in main structure type from box to sheet in terms of the shortening of the alkane chain linking the amide donor groups, the influence of the counteranions was less clear. In particular, although the 3-D networks of formula $\{[\text{M}(\text{HMBA})_3][\text{MX}_4]\}_n$ formed readily when $\text{X} = \text{Cl}$ or Br , we were unable to obtain the analogous compounds where $\text{X} = \text{I}$, although the anions MI_4^{2-} ($\text{M} = \text{Mn}, \text{Co}, \text{Ni}$) have been known for many years.² This failure prompts such considerations as whether it is a consequence of steric factors, such as the somewhat larger size of the MI_4^{2-} anions, or a diminished tendency for iodide ion transfer between these transition-metal ions under the experimental conditions employed. In terms of the latter possibility it has long been known, e.g., from spectroscopic studies,^{3–5} that

these MI_4^{2-} anions are more readily solvolyzed, even in organic solvents, than their chloro or bromo analogues.

Continued studies on related complexes with HMBA to address this matter have entailed the determination of the structures of four more complexes, $[\text{Co}(\text{HMBA})_3][\text{Co}(\text{NCS})_4]$, **1**, $[\text{Nd}(\text{HMBA})_3][\text{Nd}(\text{NO}_3)_6] \cdot 2\text{CHCl}_3$, **2**, $[\text{Co}(\text{HMBA})_3][\text{HgCl}_4]$, **3**, and $[\text{Mn}(\text{HMBA})_3][\text{HgBr}_4] \cdot 3\text{CHCl}_3$, **4**, which have not only provided a clearer understanding of the factor(s) leading to the previously observed results but also highlighted a principle which may be of wider value for the generation of other, new network materials.

Experimental Section

Preparation of Compounds. Hexamethylenebis(acetamide) was prepared as described previously.¹

Metal Complexes. $[\text{Co}(\text{HMBA})_3][\text{Co}(\text{NCS})_4]$, **1**. A solution of $\text{Co}(\text{NCS})_2$ (0.333 mmol) in ethanol (2 mL) was added to one of HMBA (1 mmol) in a hot mixture of ethyl acetate (10 mL), 2,2-dimethoxypropane (1 mL), and ethanol (1 mL). The mixture was heated to boiling, and then 12 mL of nitromethane were added. The solution was left to cool to room temperature. Deep blue crystals formed over a period of 4 d. Mp: 145–147 °C. Anal. Calcd for $\text{C}_{34}\text{H}_{60}\text{Co}_2\text{N}_{10}\text{O}_8\text{S}_4$: C, 42.9; H, 6.4; N, 14.7. Found: C, 43.2; H, 6.5; N, 14.7. IR (CsI, cm^{-1}): 3407m, 3315s [$\nu(\text{NH})$], 2072vs [$\nu(\text{NC}, \text{thiocyanate})$], 1624vs [$\nu(\text{C}=\text{O})$], 1561s [$\nu(\text{amide II})$], 1306m [$\nu(\text{amide III})$], 308s [$\nu_{11}(\text{CoN}_4)$].^{6,7}

$[\text{Nd}(\text{HMBA})_3][\text{Nd}(\text{NO}_3)_6] \cdot 2\text{CHCl}_3$, **2**. HMBA (0.55 mmol) was dissolved in a cold mixture of chloroform (4 mL) and ethanol (1 mL) and placed in a test tube. A solution of neodymium(III) nitrate hexahydrate (0.183 mmol) in acetonitrile (5 mL) was layered onto the

(3) Goodgame, D. M. L.; Goodgame, M.; Cotton, F. A. *J. Am. Chem. Soc.* **1961**, *83*, 4161.

(4) Cotton, F. A.; Goodgame, D. M. L.; Goodgame, M. *J. Am. Chem. Soc.* **1961**, *83*, 4690.

(5) Cotton, F. A.; Goodgame, D. M. L.; Goodgame, M. *J. Am. Chem. Soc.* **1962**, *84*, 167.

(6) Forster, D.; Goodgame, D. M. L. *Inorg. Chem.* **1965**, *4*, 715.

(7) Sabatini, A.; Bertini, I. *Inorg. Chem.* **1965**, *4*, 959.

(1) Goodgame, D. M. L.; Grachvogel, D. A.; Hussain, I.; White, A. J. P.; Williams, D. J. *Inorg. Chem.* **1999**, *38*, 2057.

(2) Gill, N. S.; Nyholm, R. S. *J. Chem. Soc.* **1959**, 3997.

Table 1. Crystal Data for [Co(HMBA)₃][Co(NCS)₄], **1**, [Nd(HMBA)₃][Nd(NO₃)₆·2CHCl₃], **2**, [Co(HMBA)₃][HgCl₄], **3**, and [Mn(HMBA)₃][HgBr₄·3CHCl₃], **4**

	1	2	3	4
empirical formula	C ₃₄ H ₆₀ Co ₂ N ₁₀ O ₆ S ₄	C ₃₂ H ₆₂ Cl ₆ N ₁₂ Nd ₂ O ₂₄	C ₃₀ H ₆₀ Cl ₄ CoHgN ₆ O ₆	C ₃₃ H ₆₃ Br ₄ Cl ₉ HgMnN ₆ O ₆
fw	951.02	1500.12	1002.16	1534.11
space group	<i>P</i> 1	<i>R</i> 3̄	<i>P</i> 2 ₁ / <i>c</i>	<i>P</i> 1
<i>a</i> , Å	11.528(3)	13.992(1)	16.015(2)	12.856(2)
<i>b</i> , Å	11.791(3)		14.665(1)	13.097(2)
<i>c</i> , Å	20.334(4)	25.705(2)	19.457(4)	18.002(2)
α, deg	94.01(2)			93.61(1)
β, deg	103.75(2)		101.76(1)	99.89(1)
γ, deg	111.80(2)			91.44(1)
<i>V</i> , Å ³	2454(1)	4358.3(6)	4474(1)	2978.1(7)
<i>Z</i>	2	3 ^a	4	2
ρ _{calcd} , g cm ⁻³	1.287	1.715	1.488	1.711
λ, Å	0.71073	0.71073	0.71073	0.71073
μ, mm ⁻¹	0.89	2.13	4.08	5.91
<i>T</i> , °C	20	20	20	20
<i>R</i> ₁ ^b	0.079	0.028	0.047	0.079
<i>wR</i> ₂ ^c	0.204	0.061	0.088	0.166

^a The molecule has crystallographic *S*₆ symmetry. ^b *R*₁ = Σ[|*F*_o| - |*F*_c|]/Σ|*F*_o|. ^c *wR*₂ = [Σ(*w*(*F*_o² - *F*_c²)/Σ(*w*(*F*_o²))^{1/2}], *w*⁻¹ = σ²(*F*_o²) + (*aP*)² + *bP*.

solution of HMBA. The test tube was sealed and stored at room temperature for 3 weeks, during which time large, pink crystals formed. Mp: 232–234 °C. Anal. Calcd for C₃₂H₆₂Cl₆N₁₂Nd₂O₂₄: C, 25.6; H, 4.2; N, 11.2. Found: C, 25.8; H, 4.1; N, 11.4. Electronic spectrum (reflectance, nm): 512 (⁴G_{9/2}), 524 (⁴G_{7/2}), 580 (⁴G_{5/2} + ²G_{7/2}), 675 (⁴F_{9/2}), 735br (⁴S_{3/2} + ⁴F_{7/2}), 800br (⁴F_{5/2} + ²H_{9/2}), 870 (⁴F_{3/2}). IR (CsI, cm⁻¹): 3352s [ν(NH)], 1600vs [ν(C=O)], 1566s [ν(amide II)], 1294ms [ν(amide III)].

[Co(HMBA)₃][HgCl₄], **3**. A solution of mercury(II) chloride (0.33 mmol) in warm acetonitrile (2 mL) was added to a solution of CoCl₂·6H₂O (0.33 mmol) also in acetonitrile (2 mL). This mixture was then added to a solution of HMBA (1 mmol) dissolved in a mixture of acetonitrile (8 mL), ethanol (1 mL), and 2,2-dimethoxypropane (1 mL). The resultant mixture was brought to a boil and then left to cool overnight. The following day the purple crystals which had formed were filtered off, washed with diethyl ether, and dried in vacuo. Mp: 120–122 °C. Anal. Calcd for C₃₀H₆₀Cl₄CoHgN₆O₆: C, 36.0; H, 6.0; N, 8.4. Found: C, 35.8; H, 6.0; N, 8.5. IR (CsI, cm⁻¹) 3289br,s [ν(NH)], 1626vs [ν(C=O)], 1566s [ν(amide II)], 1299m [ν(amide III)].

[Mn(HMBA)₃][HgBr₄·3CHCl₃], **4**. A solution of mercury(II) bromide (0.167 mmol) in warm acetonitrile (3 mL) was added to a solution of MnBr₂·6H₂O (0.15 mmol) in ethanol (2 mL). This mixture was then added to a solution of HMBA (0.5 mmol) dissolved in a mixture of chloroform (8 mL) and ethanol (1 mL). The resultant mixture was heated to boiling and then left to cool overnight. The following day the colorless crystals which had formed were filtered off and washed with diethyl ether. Mp: 158–160 °C. Anal. Calcd for C₃₃H₆₃Br₄Cl₉HgMnN₆O₆: C, 25.8; H, 4.1; N, 5.5. Found: C, 26.0; H, 4.1; N, 5.6. IR (CsI, cm⁻¹): 3320br,s [ν(NH)], 1625vs [ν(C=O)], 1562s [ν(amide II)], 1298m [ν(amide III)].

Microanalyses and Spectroscopic Measurements. Elemental analyses were performed by the Scientific Analysis and Consultancy Service, University of North London, and the spectroscopic measurements were made as described previously.⁸

Crystallographic Analyses. Table 1 provides a summary of the crystallographic data for compounds **1–4**. Data were collected on Siemens P4/PC diffractometers using graphite-monochromated Mo *K*α radiation. In each case the data were corrected for Lorentz and polarization factors and for absorption. The structure of **1** was solved by the heavy atom method, the rest were solved by direct methods, and the major occupancy non-hydrogen atoms were refined anisotropically using full-matrix least-squares based on *F*². Disorder was found in one of the alkyl chains in **3** and one of the solvent molecules in **4**; in each case two partial occupancy orientations were identified, with the major occupancy non-hydrogen atoms being refined anisotropically

Table 2. Selected Bond Lengths (Å) and Angles (deg) for Complex **1**

Co(1)–N(104)	1.924(9)	Co(1)–N(107)	1.952(8)
Co(1)–N(100)	1.969(8)	Co(1)–N(110)	1.976(11)
Co(2)–O(14)	2.074(5)	Co(2)–O(2)	2.077(5)
Co(2)–O(23)	2.117(5)	Co(3)–O(35)	2.062(5)
Co(3)–O(26)	2.083(6)	Co(3)–O(11)	2.114(5)
N(104)–Co(1)–N(107)	109.7(3)	N(104)–Co(1)–N(100)	108.4(4)
N(107)–Co(1)–N(100)	109.8(3)	N(104)–Co(1)–N(110)	109.0(4)
N(107)–Co(1)–N(110)	108.8(4)	N(100)–Co(1)–N(110)	111.1(4)
O(14)–Co(2)–O(2)	91.8(2)	O(14)–Co(2)–O(2)	88.2(2)
O(14)–Co(2)–O(23')	84.9(2)	O(2)–Co(2)–O(23')	85.7(2)
O(14)–Co(2)–O(23)	95.1(2)	O(2)–Co(2)–O(23)	94.3(2)
O(2)–Co(2)–O(2')	180	O(14)–Co(2)–O(14')	180
O(23)–Co(2)–O(23')	180	O(35)–Co(3)–O(26)	88.5(2)
O(35)–Co(3)–O(26')	91.5(2)	O(35)–Co(3)–O(11')	85.8(2)
O(26)–Co(3)–O(11')	85.4(2)	O(35)–Co(3)–O(11)	94.2(2)
O(26)–Co(3)–O(11)	94.6(2)	O(11)–Co(3)–O(11')	180
O(26)–Co(3)–O(26')	180	O(35)–Co(3)–O(35')	180

Table 3. Selected Bond Lengths (Å) and Angles (deg) for Complex **2**

Nd(1)–O(1)	2.318(3)	Nd(2)–O(11)	2.603(3)
Nd(2)–O(12)	2.611(3)		
O(1)–Nd(1)–O(1B)	88.06(11)	O(1)–Nd(1)–O(1A)	91.94(11)
O(1)–Nd(1)–O(1C)	180	O(11)–Nd(2)–O(11A)	68.89(6)
O(11)–Nd(2)–O(11B)	111.11(6)	O(11)–Nd(2)–O(11D)	180
O(11)–Nd(2)–O(12A)	67.93(9)	O(11A)–Nd(2)–O(12A)	48.93(9)
O(11B)–Nd(2)–O(12A)	114.29(9)	O(11C)–Nd(2)–O(12A)	65.71(9)
O(11D)–Nd(2)–O(12A)	112.07(9)	O(11E)–Nd(2)–O(12A)	131.07(9)
O(12A)–Nd(2)–O(12D)	69.02(10)	O(12A)–Nd(2)–O(12B)	110.98(10)
O(12A)–Nd(2)–O(12E)	180		

and the minor occupancy non-hydrogen atoms being refined isotropically. For all four structures the C–H hydrogen atoms of methyl groups bound to sp² centers were located from Δ*F* maps, idealized, assigned isotropic thermal parameters, *U*(H) = 1.5*U*_{eq}(C), and allowed to ride on their parent atoms. The remaining C–H hydrogen atoms were placed in calculated positions, assigned isotropic thermal parameters, *U*(H) = 1.2*U*_{eq}(C), and allowed to ride on their parent atoms. The N–H hydrogen atoms in **1** and **2** were located from Δ*F* maps and refined isotropically (fixed to *U*(H) = 1.2*U*_{eq}(N) in **1**, totally free in **2**) subject to an N–H distance constraint (0.90 Å), while those in **3** and **4** were placed in calculated positions, assigned isotropic thermal parameters, *U*(H) = 1.2*U*_{eq}(N), and allowed to ride on their parent atoms. All computations were carried out using the SHELXTL PC program system.⁹ CCDC 153372–153375.

Selected bond lengths and angles are given in Tables 2–5.

(8) Atherton, Z.; Goodgame, D. M. L.; Menzer, S.; Williams, D. J. *Inorg. Chem.* **1998**, *37*, 849.

Table 4. Selected Bond Lengths (Å) and Angles (deg) for Complex 3

Co—O(1)	2.129(5)	Co—O(2)	2.084(5)
Co—O(3)	2.061(5)	Co—O(4)	2.076(5)
Co—O(5)	2.101(5)	Co—O(6)	2.130(5)
Hg—Cl(1)	2.527(2)	Hg—Cl(2)	2.495(2)
Hg—Cl(3)	2.387(3)	Hg—Cl(4)	2.501(2)
O(3)—Co—O(4)	92.4(2)	O(3)—Co—O(2)	176.7(2)
O(4)—Co—O(2)	89.0(2)	O(3)—Co—O(5)	86.5(2)
O(4)—Co—O(5)	177.7(2)	O(2)—Co—O(5)	92.2(2)
O(3)—Co—O(1)	95.5(2)	O(4)—Co—O(1)	94.1(2)
O(2)—Co—O(1)	87.3(2)	O(5)—Co—O(1)	84.0(2)
O(3)—Co—O(6)	85.4(2)	O(4)—Co—O(6)	85.3(2)
O(2)—Co—O(6)	91.7(2)	O(5)—Co—O(6)	96.6(2)
O(1)—Co—O(6)	178.9(2)	Cl(3)—Hg—Cl(2)	121.78(9)
Cl(3)—Hg—Cl(4)	113.08(10)	Cl(2)—Hg—Cl(4)	103.01(8)
Cl(3)—Hg—Cl(1)	110.73(9)	Cl(2)—Hg—Cl(1)	98.72(7)
Cl(4)—Hg—Cl(1)	107.99(8)		

Table 5. Selected Bond Lengths (Å) and Angles (deg) for Complex 4

Hg—Br(1)	2.644(2)	Hg—Br(2)	2.598(2)
Hg—Br(3)	2.596(2)	Hg—Br(4)	2.582(2)
Mn—O(1)	2.185(10)	Mn—O(2)	2.170(9)
Mn—O(3)	2.179(8)	Mn—O(4)	2.157(11)
Mn—O(5)	2.183(10)	Mn—O(6)	2.174(10)
O(4)—Mn—O(2)	89.4(4)	O(4)—Mn—O(6)	85.7(4)
O(2)—Mn—O(6)	93.6(4)	O(4)—Mn—O(3)	93.5(4)
O(2)—Mn—O(3)	177.1(4)	O(6)—Mn—O(3)	86.7(4)
O(4)—Mn—O(5)	173.5(4)	O(2)—Mn—O(5)	84.2(4)
O(6)—Mn—O(5)	94.5(4)	O(3)—Mn—O(5)	93.0(4)
O(4)—Mn—O(1)	92.6(4)	O(2)—Mn—O(1)	89.9(4)
O(6)—Mn—O(1)	176.1(3)	O(3)—Mn—O(1)	89.9(4)
O(5)—Mn—O(1)	87.6(4)	Br(4)—Hg—Br(3)	111.25(7)
Br(4)—Hg—Br(2)	109.99(7)	Br(3)—Hg—Br(2)	115.35(7)
Br(4)—Hg—Br(1)	107.68(8)	Br(3)—Hg—Br(1)	104.13(7)
Br(2)—Hg—Br(1)	107.97(6)		

Results and Discussion

The results of the X-ray studies on compounds 1–4, taken as a set, provide the basis for assessing the role of the anions in the related HMBA complexes and, in the case of compound 2, highlight a significant and germane difference in the role of the nitrate anion from those in the polymeric structures formed by lanthanide nitrates with other uncharged “extended reach” bis-O-donor ligands of various types.^{10–12}

Structure of [Co(HMBA)₃][Co(NCS)₄], 1. Complex 1 was found to contain three independent cobalt centers. The first, Co(1), is associated with the Co(NCS)₄²⁻ anion and has the expected tetrahedral coordination geometry [N—Co—N angles in the range 108.4(4)–111.1(4)°; Co—N = 1.924(9)–1.976(11) Å]. The other two, Co(2) and Co(3), are both octahedrally coordinated to the oxygen atoms of the HMBA ligands [*cis*-O—Co—O in the range 84.9(2)–95.1(2)°; Co—O = 2.062(5)–2.117(5) Å].

There are three crystallographically independent HMBA ligands (denoted types A, B, and C), all of which have extended geometries and bridge cobalt centers of types 2 and/or 3. None of these ligands has crystallographic symmetry. The HMBA

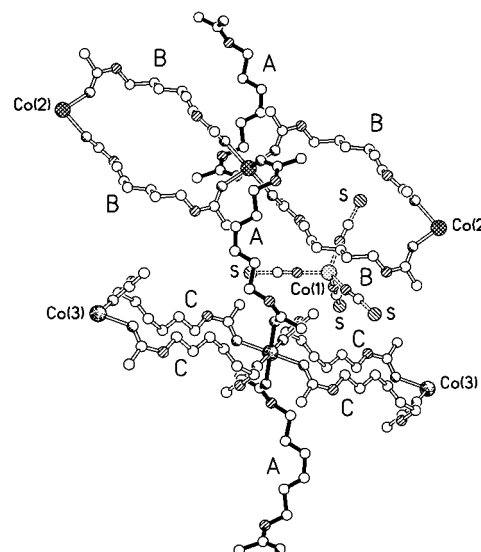


Figure 1. Part of the 3-D network of ligand-linked cobalt centers in the structure of 1, showing the linking by HMBA ligands of type A of approximately orthogonally arranged 26-membered macrocycles, and also the Co(NCS)₄²⁻ anion.

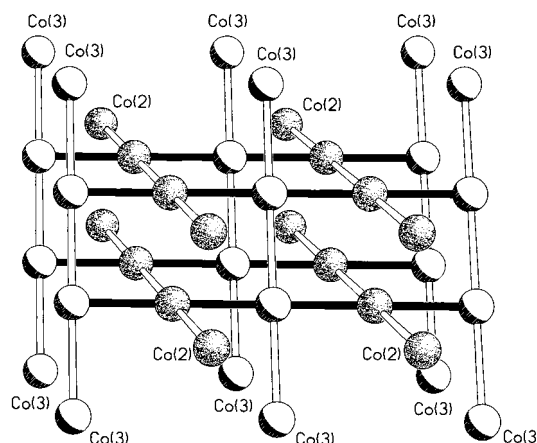


Figure 2. Schematic representation of the linking of the independent cobalt centers to form a 3-D network in 1. The heavy “bonds” correspond to the linking by ligands of type A.

ligands of type B each form pairs of bridges between the equatorial coordination sites of type 2 cobalt centers to form chains of 26-membered macrocycles. The HMBA ligands of type C bridge cobalt centers of type 3 in the same fashion to generate analogous chains of 26-membered macrocycles that are oriented approximately orthogonally to those formed by Co(2) and HMBA ligands of type B. Both of these types of macrocycles have crystallographic inversion symmetry. These sets of chains are then cross-linked via single strands of HMBA ligands of type A which bridge the metal centers by coordinating to the remaining, axial sites on each metal (Figure 1).

The combined effect of these three types of bridging actions is to form a contiguous 3-D network of a type we have not observed previously. In the structure of [Co(HMBA)₃][Co(NCS)₄] we see approximately rectangular and parallel lattices formed, for example, by cobalt centers of type 3 being linked by cobalt centers of type 2 that reside at the midpoints of their long edges. Each cobalt atom can thus be envisaged as being in a pseudo “square planar” environment with respect to its nearest neighbors (Figure 2). Within this lattice the long and the short edges of the rectangle formed by cobalts of type 3 are

- (9) SHELXTL PC, version 5.03, Siemens Analytical X-ray Instruments Inc., Madison, WI, 1994.
- (10) Goodgame, D. M. L.; Hill, S. P. W.; Williams, D. J. *Polyhedron* **1993**, *12*, 2993. Goodgame, D. M. L.; Menzer, S.; Ross, A. T.; Williams, D. J. *Inorg. Chim. Acta* **1996**, *251*, 4245. Goodgame, D. M. L.; Menzer, S.; Smith, A. M.; Williams, D. J. *Chem. Commun.* **1997**, 339 and references therein.
- (11) Zhang, R. H.; Ma, B. Q.; Bu, X. H.; Wang, H. G.; Yao, X. K. *Polyhedron* **1997**, *16*, 1123.
- (12) Goodgame, D. M. L.; Hill, S. P. W.; Williams, D. J. *Inorg. Chim. Acta* **1998**, *272*, 4245.

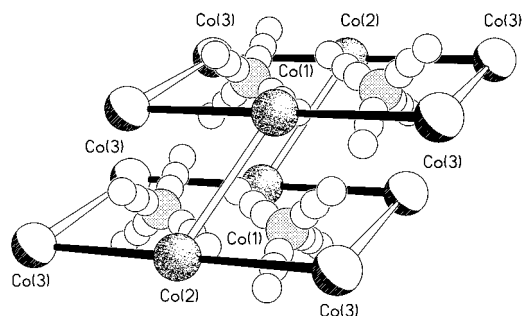


Figure 3. Disposition of the $\text{Co}(\text{NCS})_4^{2-}$ anions within the network present in the structure of **1**.

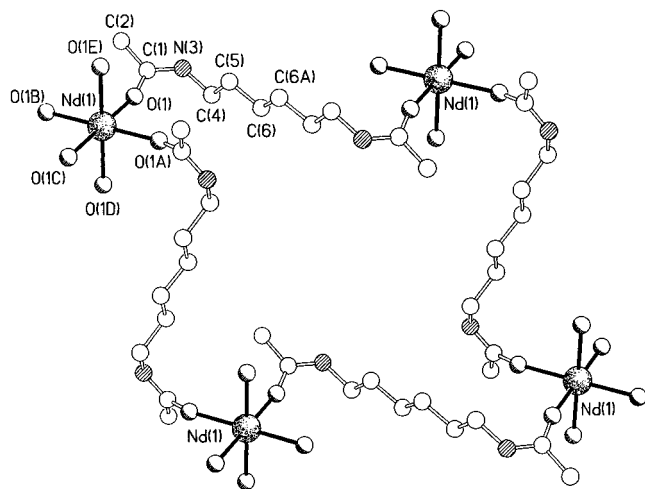


Figure 4. One of the 52-membered ring systems present in the polymeric structure of **2**.

22.78 and 13.08 Å, respectively, and the center edge links between cobalts of type 2 are 11.79 Å.

The $\text{Co}(\text{NCS})_4^{2-}$ anions reside within the rectangular “windows” of this network as depicted in Figure 3. The only anion–cation interaction of note is the directing of the HMBA ligand N–H protons toward the anion sulfur atoms. Three of the four sulfur atoms have $\text{S}\cdots\text{N}$ contacts in the range 3.42–3.51 Å.

Structure of $[\text{Nd}(\text{HMBA})_3][\text{Nd}(\text{NO}_3)_6]\cdot 2\text{CHCl}_3$, **2.** The X-ray study of compound **2** shows it to have the composition $[\text{Nd}(\text{HMBA})_3][\text{Nd}(\text{NO}_3)_6]\cdot 2\text{CHCl}_3$ comprising a cationic framework of octahedrally coordinated neodymium centers, Nd(1), bridged by HMBA ligands (Figure 4), to form a network of 52-membered macrocycles and containing $[\text{Nd}(\text{NO}_3)_6]^{3-}$ counteranions.

The symmetry at each of the Nd(1) centers is S_6 , and the distortions from O_h symmetry are small, the *cis* angles being 88.06(11)° and 91.94(11)° and all the Nd–O distances 2.318–(3) Å. Within the rhombus illustrated in Figure 4, the linked Nd–Nd centers are separated by 11.78 Å, while the transannular separations are 13.99 and 18.95 Å, respectively. This motif then extends in three dimensions to create a network (Figure 5) that is directly analogous to that formed by nickel(II) in the nickel perchlorate complex with *N,N'*-*m*-phenylenedimethylenebis(pyridin-2-one).¹³ As was found for that nickel complex,¹³ the network contains large voids within which are located the counteranions. In compound **2** these anions are $[\text{Nd}(\text{O}_2\text{NO})_6]^{3-}$, containing six chelating nitrate groups, and which have been formed by complete nitrate ion transfer from half of the original neodymium nitrate starting material.

Although there is a distinct “waisting” of the central region of the cavity such that all of the bounding amide groups have their N–H bonds directed inward toward the anion, there are, surprisingly, no strong $\text{N–H}\cdots\text{O}$ hydrogen bonds formed; the shortest $\text{H}\cdots\text{O}$ distance is 2.50 Å. As a consequence of the waisting process, secondary cavities are created “above” and “below” the anion, and these are filled by the chloroform solvent molecules, which, again, are not involved in any strong intermolecular interactions. Despite the absence of dominant anion/framework/solvent interactions, the resultant material is remarkably compact.

Structure of $[\text{Co}(\text{HMBA})_3][\text{HgCl}_4]$, **3.** The solid complex formed by reacting HMBA with a 1:1 mixture of cobalt(II) chloride and mercury(II) chloride in a mixture of acetonitrile, ethanol, and 2,2-dimethoxypropane has the stoichiometry $\text{CoHgCl}_4(\text{HMBA})_3$. The X-ray study of this compound shows that each cobalt atom is coordinated to six HMBA ligands with a nearly octahedral coordination geometry (Figure 6), the Co–O distances and *cis*–O–Co–O angles being in the ranges 2.061–(5)–2.130(5) Å and 84.0(2)–96.6(2)°, respectively.

There are five crystallographically unique HMBA ligands, four of which (B, C, D, and E in Figure 6) have inversion symmetry while the fifth (A) occupies the remaining two coordination sites. All of the HMBA ligands bridge to adjacent cobalt centers to form ruckled 2-D sheets (Figure 7) comprising contiguous three-sided 39-membered macrocycles. Within each sheet there are two distinct types of 39-membered macrocycles, one being bounded by HMBA ligands of types A, B, and C, whereas the other has edges formed by HMBA ligands of types A, D, and E. The HgCl_4^{2-} anions are sandwiched between adjacent sheets but are offset such that one of the coordinated Cl atoms, Cl(3), is inserted through the center of one of the macrocycles (that bounded by HMBA ligands of types A, D, and E) whereas the remaining three, basal Cl atoms, Cl(1), Cl(2), and Cl(4), are positioned over the center of the other type of macrocycle, namely, that bounded by ligands of types A, B, and C. Adjacent sheets are cemented together by $\text{N–H}\cdots\text{Cl}$ hydrogen bonds (a–f in Figure 8) which utilize the donor capacities of all six unique amide N–H groups.

Structure of $[\text{Mn}(\text{HMBA})_3][\text{HgBr}_4]\cdot 3\text{CHCl}_3$, **4.** A reaction essentially analogous to that which produced the crystals of compound **3**, but using mercury(II) bromide and manganese(II) bromide and HMBA in a mixture of acetonitrile, chloroform, and ethanol, afforded colorless crystals of compound **4** of stoichiometry $\text{HgMnBr}_4(\text{HMBA})_6\cdot 3\text{CHCl}_3$. The X-ray analysis of **4** shows that, as in **3**, there are five crystallographically unique HMBA ligands, four of which again have inversion symmetry. The coordination geometry at manganese is again slightly distorted octahedral, with Mn–O distances ranging between 2.157(11) and 2.185(10) Å (Figure 9). Despite these features in common with **3**, the network generated is subtly different. As in **3**, all five unique HMBA ligands bridge to adjacent Mn centers. However, here 2-D sheets are formed that comprise a combination of both three-sided 39-membered and four-sided 52-membered ring systems arranged contiguously (Figure 10). The three-sided rings are formed by ligands of types A, B, and D, whereas the four-sided rings are centrosymmetric and are formed by ligands of types A and C only.

Also, unlike **3**, where the supramolecular arrangement is of the form of parallel sheets cross-linked by $\text{N–H}\cdots\text{Cl}$ hydrogen bonds to the interstitial HgCl_4^{2-} anions, here in **4** there is a covalently linked 3-D network in which HMBA ligands of type E form intersheet connectors instead of partitioning each four-sided macrocycle (to form pairs of three-sided rings, as in **3**).

(13) Goodgame, D. M. L.; Menzer, S.; Smith, A. M.; Williams, D. J. J. *Chem. Soc., Chem. Commun.* **1994**, 1825.

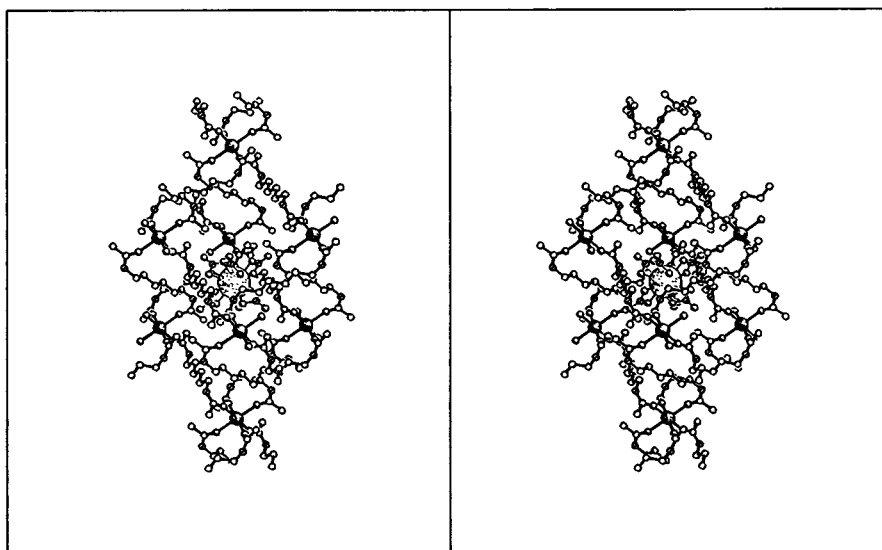


Figure 5. Stereoscopic representation of part of the 3-D network present in **2** also showing one of the included $\text{Nd}(\text{NO}_3)_6^{3-}$ anions.

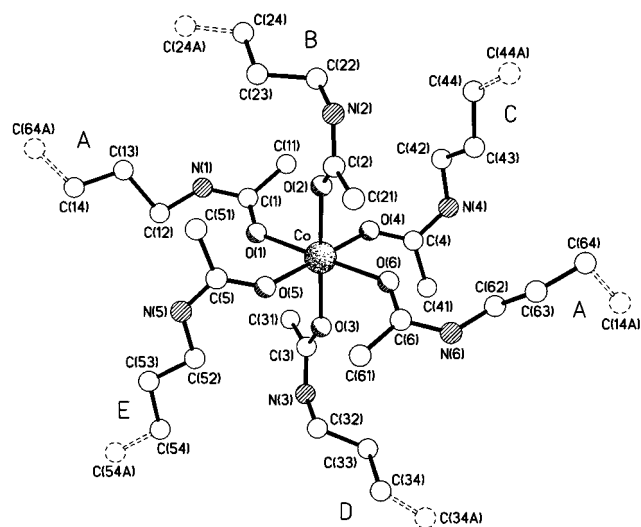


Figure 6. Cobalt environment in the structure of **3** showing the five independent ligand types A–E.

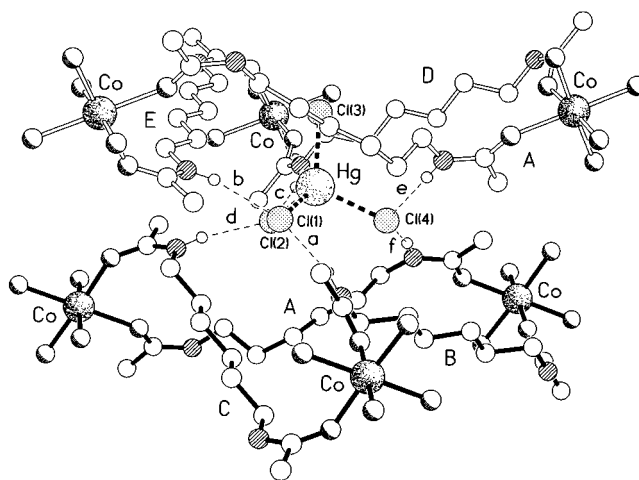


Figure 8. Positioning of the HgCl_4^{2-} anions between the sheets in **3** and the directing of one of the Hg–Cl bonds through the ADE-type ring. The hydrogen-bonding geometries, $\text{N}\cdots\text{Cl}$ (Å), $\text{H}\cdots\text{Cl}$ (Å), $\text{N}-\text{H}\cdots\text{Cl}$ (deg), are (a) 3.21, 2.33, 167, (b) 3.27, 2.38, 168, (c) 3.19, 2.34, 156, (d) 3.27, 2.38, 170, (e) 3.34, 2.44, 176, and (f) 3.43, 2.55, 165.

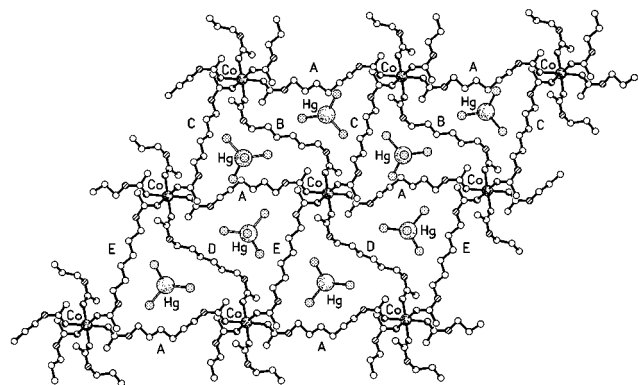


Figure 7. Part of one of the ruckled 2-D sheets of fused 39-membered rings of two distinct types (ABC and ADE). The relative positions of the HgCl_4^{2-} anions are also depicted.

The 3-D network thus formed can still be regarded as cross-strutted parallel sheets with, in this case, the HgBr_4^{2-} anions intercalated between them (Figure 11). Here, however, the anions are not offset and do not insert their bromine atoms into the rings that comprise the sandwiching sheets, though there are $\text{N}-\text{H}\cdots\text{Br}$ hydrogen bonds (a–f in Figure 11) between all

of the unique amide N–H groups and the bromine atoms. The three chloroform solvent molecules per Mn center that are present in this structure are also intercalated between the principal sheets.

Conclusions

The main conclusion to be drawn from the set of structures described above is the importance of the intermetal transfer of the “simple” anions (viz., Cl^- , Br^- , NCS^- , or NO_3^-), thus facilitating the formation both of the octahedrally coordinated (MO_6) “node” points of the HMBA-linked cationic frameworks and of the more highly charged complex counteranions of appropriate sizes and shapes to occupy the framework “voids”.

This factor is particularly noteworthy in the structure of compound **2**. By linking the bridged Nd centers, the resulting array comprises a network of contiguous rhomboidal boxes with the anions located at their centers. Although polymeric structures have been reported for lanthanide nitrate complexes with a wide range of other uncharged “extended reach” O-donor ligands,^{10–12} they have, so far as we are aware, retained either two or all three of the nitrate anions directly coordinated to the metal

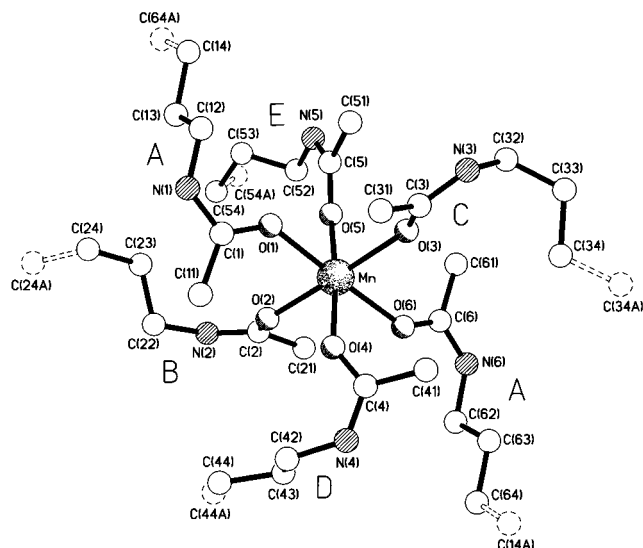


Figure 9. Manganese coordination environment in the structure of **4** showing the five ligand types A–E.

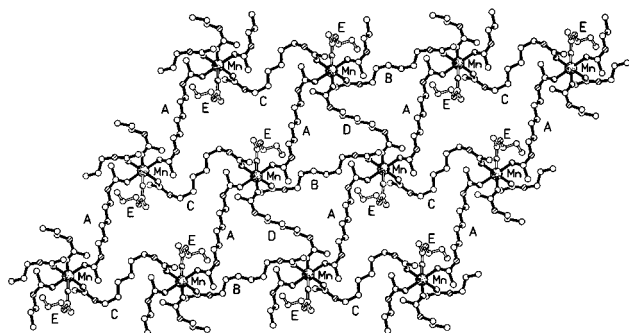


Figure 10. Part of one of the sheets of linked 39- and 52-membered macrocycles present in the 3-D polymer structure of **4**.

centers. In **2**, however, the HMBA ligands have completely displaced the nitrates from the coordination sphere of the Nd atoms forming the network, thus generating the charge-balancing $[\text{Nd}(\text{NO}_3)_6]^{3-}$ anions and a compact array.

The ready formation of the network structure of $\{[\text{Co}(\text{HMBA})_3][\text{Co}(\text{NCS})_4]\}_n$ (compound **1**), in contrast to our previous failure to isolate an analogous complex $\{[\text{Co}(\text{HMBA})_3][\text{CoL}_4]\}_n$, using essentially similar reaction conditions, also implies that anion size is not per se a determining factor, but rather reflects the relative lability of the CoL_4^{2-} anion, as noted earlier.

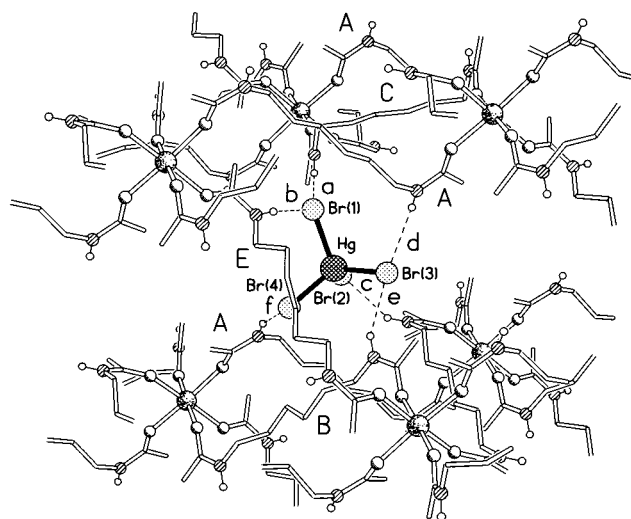


Figure 11. Location and hydrogen bonding of the HgBr_4^{2-} anion between the “sheets” present in the structure of **4** and also the cross-linking of the sheets by ligands of type E. The hydrogen-bonding geometries, $\text{N}\cdots\text{Br}$ (Å), $\text{H}\cdots\text{Br}$ (Å), $\text{N}-\text{H}\cdots\text{Br}$ (deg), are (a) 3.37, 2.53, 154, (b) 3.42, 2.58, 168, (c) 3.52, 2.72, 148, (d) 3.64, 2.88, 143, (e) 3.66, 2.82, 156, (f) 3.48, 2.64, 156.

The structures of compounds **3** and **4** demonstrate that by harnessing the established principle of inter-metal-anion transfer one can achieve a measure of selectivity in the nature of the metal network node points and the counteranion(s). In these examples we have simply exploited the difference in “hardness/softness” character between cobalt(II) or manganese(II) and mercury(II), but we conjecture that, by appropriate choice of metals, “simple” anions, and donor atoms on the bridging, extended-reach ligands, it should be possible to generate new, preprogrammed types of network array complexes.

Acknowledgment. We thank the EPSRC for a Research Studentship (to D.A.G.) and for equipment. I.H. thanks the Commonwealth Scholarship Commission for a fellowship and the University of Balochistan, Pakistan, for a leave of absence.

Supporting Information Available: X-ray crystallographic files in CIF format for the structure determinations of $[\text{Co}(\text{HMBA})_3][\text{Co}(\text{NCS})_4]$, **1**, $[\text{Nd}(\text{HMBA})_3][\text{Nd}(\text{NO}_3)_6]\cdot 2\text{CHCl}_3$, **2**, $[\text{Co}(\text{HMBA})_3][\text{HgCl}_4]$, **3**, and $[\text{Mn}(\text{HMBA})_3][\text{HgBr}_4]\cdot 3\text{CHCl}_3$, **4**. This material is available free of charge via the Internet at <http://pubs.acs.org>.

IC000673I